

Application of VITA technique for detection of the organized structures present in a turbulent boundary layer under an adverse pressure gradient

A. DRÓŹDŹ, W. ELSNER, S. DROBNIAK

*Institute of Thermal Machinery
Czestochowa University of Technology
Al. Armii Krajowej 21
42-201 Czestochowa, Poland
e-mails: arturdr@imc.pcz.czyst.pl,
welsner@imc.pcz.czyst.pl,
drobniak@imc.pcz.czyst.pl*

THE PAPER CONCERNS experimental investigations of turbulent boundary layer (TBL), developing on a flat plate at $Re_\theta = 3000$ under an adverse pressure gradient (APG) corresponding to the case of pressure variation at axial compressor blading. In particular, the paper deals with the analysis of bursting phenomena and coherent structures activity in TBL with the use of VITA technique. The interpretation of coherent structures was based on the analysis of conditionally averaged traces of u and v velocity components recorded by X-wire probe in several boundary layer regions. The paper describes the modification introduced into the VITA method, which enables to distinguish four types of coherent structures. This modification relies on the detection of instantaneous positive or negative gradients of u and v velocity traces. It was found that bursting process under the influence of adverse pressure gradient is damped near the wall and this phenomenon is even more pronounced in the outer region of turbulent boundary layer. Furthermore, the paper gives the consistent proof, that vortices developing in TBL create the effect of bursting present in velocity signal.*)

Key words: turbulent boundary layer, VITA technique, bursting phenomena, adverse pressure gradient.

Copyright © 2011 by IPPT PAN

Notations

β Clauser pressure parameter,
 H shape factor,
 δ^* displacement thickness,
 k detection level,
 L test section length,
 N number of structures,
 p_∞ static pressure of the free-stream,

*)The paper was presented at 19th Polish National Fluid Dynamics Conference (KKMP), Poznań, 5–9.09.2010.

Re_θ	Reynolds number based on momentum thickness,
S_g	dimensionless distance from inlet plane $S_g = x_s/L$,
t	time,
T	time averaging window,
Tu	turbulence intensity of the free stream $Tu = u/U_0$,
τ	phase averaging time,
τ_w	wall shear stress,
θ	momentum thickness,
U, V	mean velocity components in x and y directions,
u_τ	friction velocity,
u^+	dimensionless velocity $u^+ = U/u_\tau$,
u, v	fluctuating velocity components in x and y directions,
u', v'	rms values of fluctuating velocity components in x and y directions,
ν	kinematic viscosity,
x, y, z	streamwise, wall-normal and spanwise coordinates,
x_s	longitudinal distance from inlet plane,
y^+	dimensionless distance from the wall in inner scaling,
$\langle \rangle$	conditional averaging,
$+$	inner scale symbol.

Abbreviations

rms	root mean square,
TBL	Turbulent Boundary Layer,
APG	Adverse Pressure Gradient,
VITA	Variable Interval Time Averaging.

1. Introduction

RECENT EXPERIMENTAL AND COMPUTATIONAL STUDIES [13] suggest, that significant part of wall turbulence could be described in terms of deterministic structures. The near-wall region is characterised by the presence of low-speed streaks and hairpin vortices that are being assembled into large-scale coherent groups named vortex packets. These structures are qualitatively consistent with the horseshoe vortex model proposed by TEODORSEN [2]. The oscillation and then the break-up of these structures, known as bursting phenomena, cause high gradients of velocity both in time and in space. KIM *et al.* [3] found that the bursting process, which produces roughly 70% of total turbulence, is a result of break-up of shear layer caused mainly by ejection events in a buffer layer. Subsequently, CORINO and BRODKEY [4] proved that this event was closely related to sweep event that is a large-scale motion towards the wall.

In 1976 BLACKWELDER and KAPLAN [1] developed the VITA (Variable Interval Time Averaging) technique, where a localized measure of the turbulent kinetic energy was proposed and used to detect rapid changes in velocity time signal. Later on, VITA detection scheme was modified by adding a slope condition to distinguish between rapid acceleration and deceleration [12]. This modification allowed to distinguish between the positive/negative detections.

In the following years this scheme became one of the most commonly applied methods for the detection of structures, which are responsible for the bursting process present in TBL. According to ADRIAN *et al.* [11], the main VITA detections can be interpreted as the tilted shear-layers passage through the measuring point location, where rapid acceleration of u velocity component and rapid deceleration of v velocity component occur. However, one should be aware that VITA method allows only to detect the break-up of large-scale motions into smaller scales, characterised by high gradients of a velocity signal. That is why the large-scale motions, i.e. ejection and sweep, could not be identified directly with VITA method. This limitation may be eliminated by combination of the VITA method with other signal processing techniques.

This methodology combined with quadrant analysis was applied by several authors, e.g. ADRIAN [5], to the analysis of streamwise and normal velocity components and it allowed to explain the origin of bursting process. Quadrant analysis is commonly used to describe a relation of u and v velocity components in xy plane. The velocity time-courses recorded in the xy plane are divided into four quadrants, where four events commonly named $Q1$, $Q2$, $Q3$ and $Q4$ exist. Velocity components take positive u and v values for the first quadrant ($Q1$ event), a negative u and positive v for the second quadrant ($Q2$ event), a negative u and v for the third quadrant ($Q3$ event) and a positive u and negative v for the fourth quadrant ($Q4$ event). It means that VITA technique combined with quadrant analysis allows to identify bursting process, i.e. enables to distinguish between the effect of sweep in $Q4$ and ejection in $Q2$ quadrants.

The interpretation of bursting phenomena presented above was proposed for the zero pressure gradient turbulent boundary layer. From the viewpoint of practical application, more important is the knowledge of transport processes in the turbulent boundary layer subjected to the impact of pressure gradient and especially, the adverse pressure gradient (APG). This research was intensified in the recent period, but most of previous investigations on APG TBL concerned the analysis of global characteristics, including scaling problems [9].

One of the pioneering papers devoted to analysis of the behaviour of organised structures present in a boundary layer subjected to adverse pressure gradient is a work of KROGSTAD and SKARE [7], who performed investigations with the help of hot-wire measurements, two-point correlation analysis and quadrant decomposition. Their analysis of uv Reynolds shear stresses allowed to conclude, that the APG flow was strongly dominated by turbulent motions towards the wall ($Q4$ events) in contrast to zero pressure gradient flow, where both $Q2$ and $Q4$ events were equally important. KROGSTAD and SKARE [7] did not give the explanation of the origin of such a change in the $Q2$ and $Q4$ distributions, however, they provided the evidence that in the case of strong events, the considerable

contribution from outward interactions was observed in the first quadrant ($Q1$). It is worth to note that identification process based on uv parameter allowed to distinguish between $Q2$ (ejection) and $Q4$ (sweep) events, but these conclusions were only qualitative. The detailed, quantitative description of transport processes could not be obtained, because the events detected from uv signal could be a result of the joint impact from various types of vortical structures, which were present in TBL.

As it will be shown later, within the TBL various types of structures are present, with either positive or negative vorticity, which in addition move upwards or downwards and for the proper identification of these structures, the slope detection function in VITA should be applied to u and v velocity components simultaneously. Such a method of signal processing proposed in the present paper, supplemented by combination of VITA technique with quadrant decomposition, should allow to identify various types of vortices passing through the measuring point with different rotation directions, various directions of motion and various convection velocities. These features of the proposed signal processing technique, together with its application to the TBL under the streamwise pressure gradient, are the novel elements of the paper.

2. Experimental conditions and apparatus

The experimental investigations of the TBL under APG for to $Re_\theta \approx 3000$ were performed in an open-circuit wind tunnel shown in Fig. 1, where the turbulent boundary layer developed along the flat plate, which was 2807 mm long and 250 mm wide (the details of experimental rig and measuring procedures may be found in [8]). The upper wall was shaped according to the assumed distribution of pressure gradient shown in Fig. 2, which corresponded to the conditions encountered in stator passages of turbomachinery.

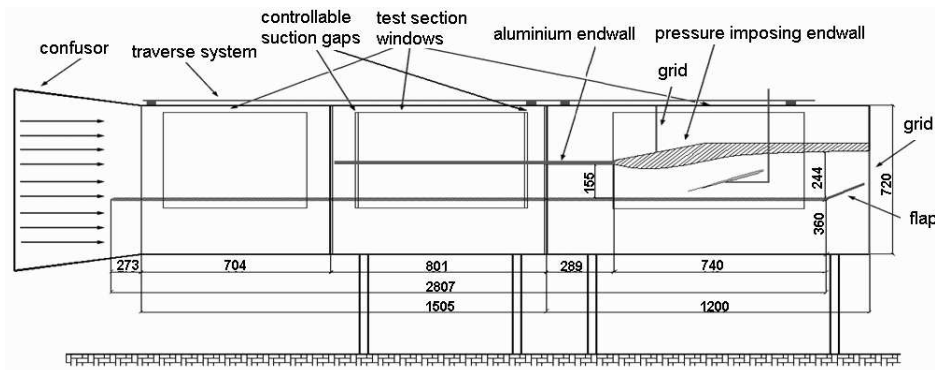


FIG. 1. Schematic view of the wind tunnel and measuring test section.

The velocity at the inlet plane outside the boundary layer was 15 m/s, while the turbulence intensity was equal $Tu \approx 0.4\%$. In the experiment, a tripping of boundary layer after the leading edge of a flat plate was applied, which allowed to obtain a relatively high value of characteristic Reynolds number.

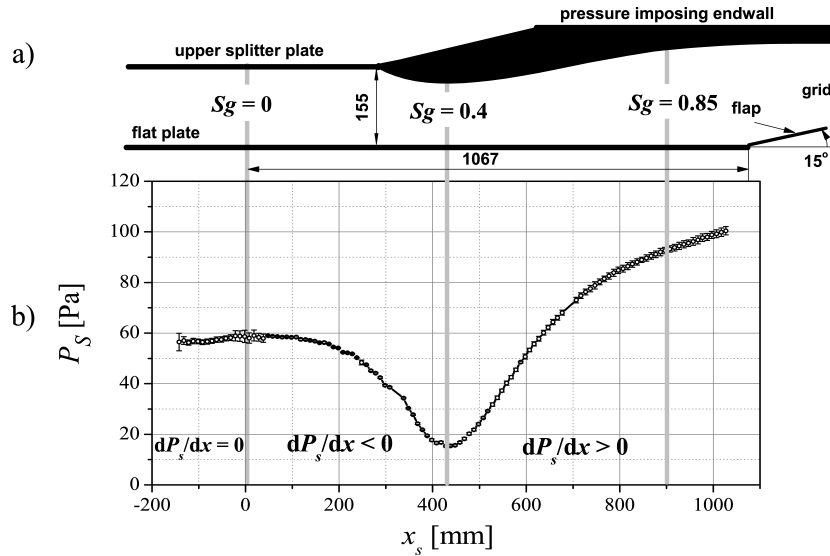


FIG. 2. The shape of upper wall: a) and the corresponding static pressure distribution, b) along the flat plate.

The static pressure distribution (Fig. 2) was measured at the flat plate with DATA INSTRUMENTS DCXL01DN pressure transducer connected to KULITE D486 amplifier. The mean relative error of pressure measurements was equal to 2.67% for APG region. Two velocity components were measured in several cross-sections of APG region with X-wire probe (Dantec Dynamics 55P52). The X-wire probe with the wire diameter $d = 5 \mu\text{m}$ and the length $l = 1.25 \text{ mm}$ was combined with the DISA 55M hot-wire anemometer connected to 12 bit PC card. Acquisition was maintained at frequency 25 kHz with 10 seconds sampling records. Due to large measuring volume, the probe could not penetrate the boundary layer below $y^+ < 20$. For the purpose of the current investigation, four

Table 1. Location and characteristic parameters for measuring cross-sections.

x_s [mm]	S_g	u_τ [m/s]	dp_∞/dx
487	0.456	0.708	0.208
577	0.541	0.564	0.267
667	0.625	0.449	0.190
787	0.738	0.338	0.099

cross-sections listed in Table 1 were chosen. Within this range of the x_s distances from the leading plane (Table 1), the shape factor H increased linearly from 1.3 to 1.7 and Clauser pressure parameter $\beta = \delta^*/\tau_w(dp_\infty/dx)$ increased linearly from value 1 to 7.

3. VITA method and process of vortex structure detection

The VITA detection scheme is based on the analysis of a running variance $\text{var}(t, T)$ of detection parameter $a(t)$ given by equation:

$$(3.1) \quad \text{var}(t, T) = \frac{1}{T} \int_{t-T/2}^{t+T/2} a(t')^2 dt' - \left[\frac{1}{T} \int_{t-T/2}^{t+T/2} a(t') dt' \right]^2.$$

Parameters of the detection process were properly tuned in order to obtain the best possible efficiency of the procedure. It was decided that the detection parameter $a(t)$ would be a streamwise velocity signal u which gives higher amplitudes of velocity fluctuations in comparison with normal to the wall v component of velocity. Then signs of derivatives du/dt and dv/dt were analysed to apply quadrant analysis and to distinguish between four possible structures discussed later. An important parameter was also a time averaging window T which should be related to the scale of dominant structure. In order to select the appropriate time averaging window T , the maximum number of positive vorticity ascending structures N was used. The number of those structures was significantly larger in comparison with others and furthermore the peak of $N(T)$ distribution was more pronounced, which allowed to select the optimum value of T with less ambiguity. The next important parameter of VITA technique was the threshold value $k(u')^2$ of detection function $D(t, T)$. For a current research a dual slope method [10] for $N(k)$ distribution was applied with good effect. The steps of VITA procedure are presented in Fig. 3 which includes velocity signals (top), the corresponding short time variance (center), and the detection function (bottom).

During the preliminary analysis it was found that the original VITA method does not give the accurate time location of the structure centre, especially when two structures are very close to each other. To improve structure centering process, the calculation of centre point between maximum and minimum of smoothed velocity time traces was introduced. This additional procedure substantially improved the phase averaging and also the slope detection processes. Slope detection function $D(t)$ takes the following values: $\{-2, -1, 1, 2\}$. Sign in the detection function describes the slope of gradients of u velocity component during detection, values 1 and 2 correspond to ascending and descending vortices respectively.

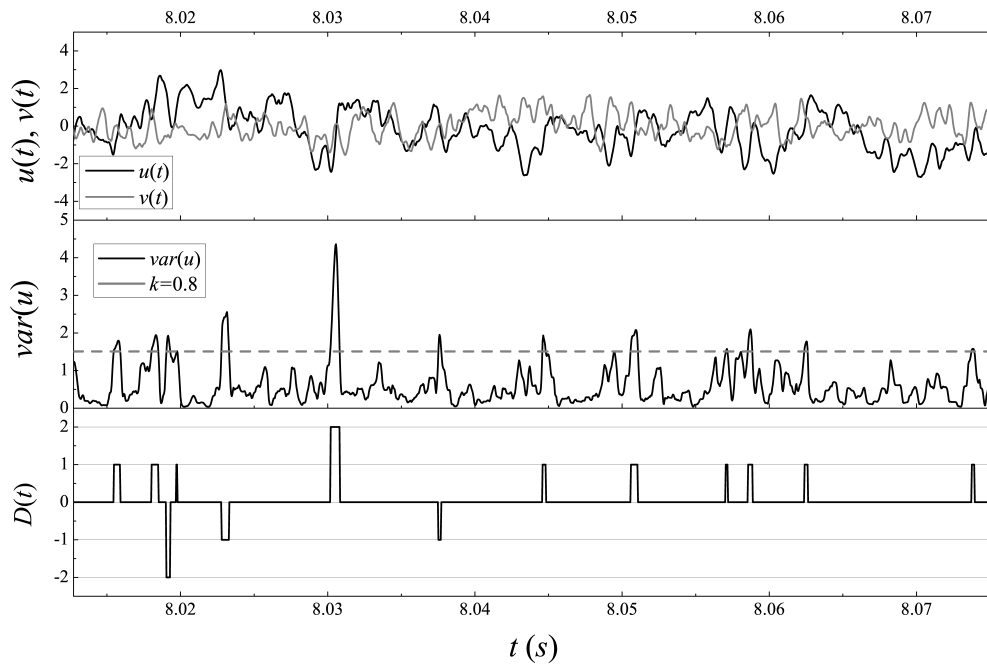


FIG. 3. From the top: time series for the u and v velocity components at $y^+ = 46.5$, the short time variance $\text{var}(u)$ with integrating window $T^+ = 26$, detection function $D(t)$ for $k = 0.8$.

The structure characterised by positive gradient (+) of u and negative gradient (−) of v velocity components, which is marked as (+−), can be interpreted as the so-called “retrograde” (positive vorticity) vortex [6] passing through the sensor in the direction from $Q3$ to $Q1$ quadrant. The VITA also detects negative gradients (−) of u and positive gradient (+) of v velocity components, marked as (−+), which are the effect of prograde (negative vorticity) vortex passing through the sensor. This approach allows to recognise two possible vortical structures in xy plane, i.e. prograde spanwise vortex with rotation direction the same as dU/dy and retrograde spanwise vortex with rotation direction opposite to dU/dy . For those vortical structures two convection directions exist i.e. ascending (moving away from the wall) and descending (moving towards the wall). When vortex center passes through the measuring point, the measured resultant velocity vector is perpendicular to the direction of the vortex motion. When retrograde ascending vortex passes through the measuring point then $Q2$ event appears before and $Q4$ event after the vortex center, while for the prograde ascending vortex the events change their order. For the ascending vortices their velocity components are in opposite phase and give negative Reynolds stresses $-uv$ (i.e. $Q2$ and $Q4$ events). Because most of the vortices are moving away from the wall, the negative Reynolds stress prevails in the turbulent boundary layer

hot-wire signals. When retrograde descending vortex passes through the measuring point, then $Q1$ event appears before and $Q3$ after the vortex center, while for prograde descending vortex the events change their order. When descending vortex passes through the measuring point their velocity components are in phase and give positive Reynolds stress uv (resulting from $Q1$ and $Q3$ events).

In order to characterise four possible VITA structures described above, the sample time traces of phase-averaged velocities $\langle u \rangle$ and $\langle v \rangle$ for a normalized coordinate $y^+ \approx 20$ from the first cross-section are presented in Fig. 4. Identified retrograde vortical structures are shown in Fig. 4a and prograde ones in Fig. 4b. Distributions of the $\langle u \rangle$ and $\langle v \rangle$ are approximately 180° out of phase for ascending structures (black colour) and in phase for descending ones (grey colour). Rotation directions at the schemes indicate the type of vortex, while arrows show the vortex passage directions through the sensor location.

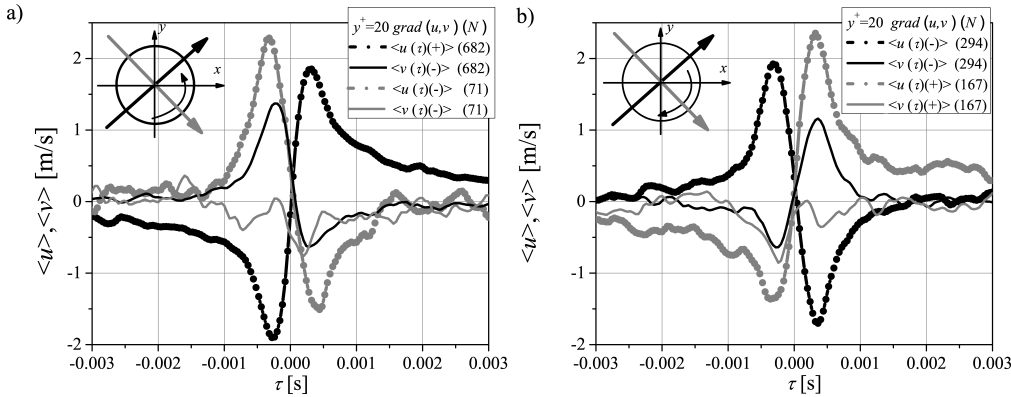


FIG. 4. Phase averaged velocities during detections and schemes of the vortex passage directions: a) retrograde, b) prograde; number of detected structures (N) in brackets.

The conditionally averaged distributions of velocity components also confirm ascending or descending character of vortex movement. One may notice that the time courses of both $\langle u \rangle$ and $\langle v \rangle$ velocity components are not symmetrical with respect to the τ axis. If the average value of $\langle u \rangle$ course is shifted upwards, it means that vortex moves faster than the surrounding mean flow in the given direction, the opposite denotes a slower vortex motion with respect to the mean flow. It is seen in Fig. 4 that for descending vortices, the distribution of $\langle u \rangle$ velocity component is shifted towards positive values and $\langle v \rangle$ is shifted towards negative ones, which confirms that descending structure arrives from a higher momentum zone (i.e. from a higher position in the boundary layer). The opposite situation is visible for ascending structures.

One can observe that the retrograde ascending vortex has the same positive gradient of u velocity component as the prograde descending one. The difference

between those vortices is only in dv/dt . If the slope condition in VITA detection scheme were based on u velocity only, then for positive gradient du/dt both the retrograde and prograde vortices would be averaged together. In such a case, the phase averaged distributions of v component would be distorted, because two portions of the signal with opposite gradients would be averaged together.

4. Mean flow characteristics

The detailed analysis of flat plate turbulent boundary layer performed by DROBNIAK *et al.* [9] showed that the adverse pressure gradient induced a rapid build-up of boundary layer, which was accompanied by the decrease of wall shear stresses. It should be noticed however, that the pressure gradient applied in [9] was not strong enough to induce a boundary layer separation. It was also demonstrated that the near-wall region grew much more slowly than the outer part of the boundary layer what in turn implied that most of the contribution to APG boundary layer growth originated from areas located far from the wall. The same conclusion may also be found from the distribution of Reynolds stresses (Fig. 5), which may be treated as an indirect indication of intensity of turbulent trans-

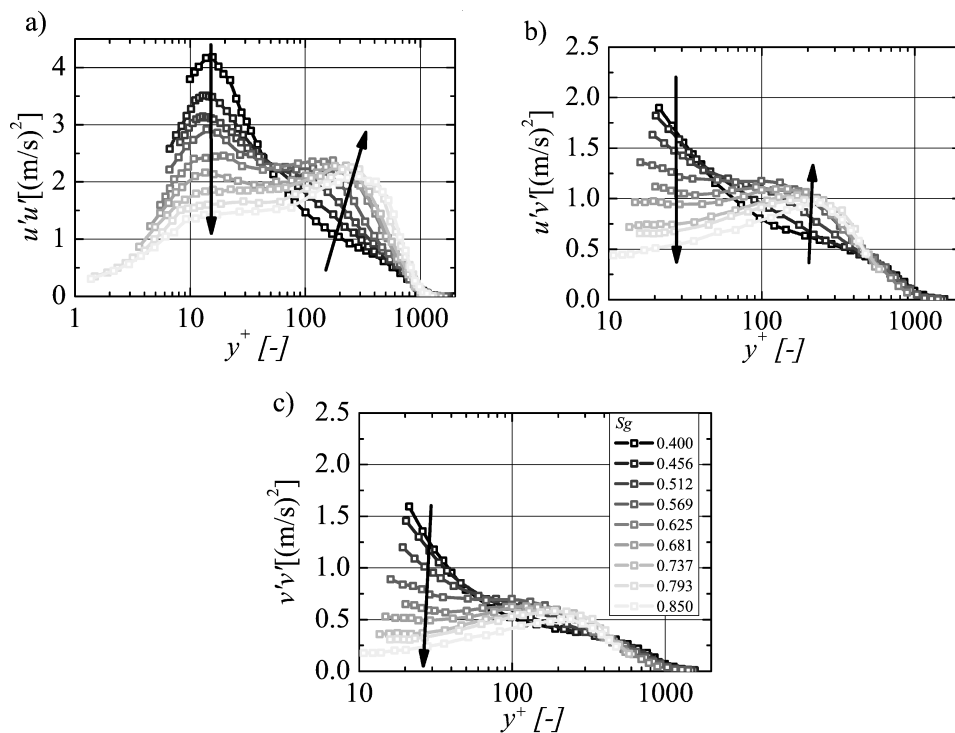


Fig. 5. Reynolds stresses in xy plane in y^+ coordinates. Arrows indicate the change along the flow in APG conditions of: a) $u'u'$ normal stresses, b) $u'v'$ shear stresses, c) $v'v'$ normal stresses.

port. Analysis of Reynolds normal $u'u'$, $v'v'$ and shear stresses $u'v'$ distributions, shown in Fig. 5, reveals in the first cross-section the existence of a single maximum located in the immediate vicinity of the wall ($y^+ \approx 15$), which gradually decays in the downstream area.

At the same time, the outer maximum located at $y^+ \approx 200$ appears and becomes the more pronounced, the further downstream is the location of the measuring cross-section (arrows in Fig. 5 denote the decay and appearance of inner and outer maxima respectively). It means therefore that in presence of APG, the appearance of second peak of turbulent velocity fluctuations confirms the more pronounced contribution of outer region to the downstream development of TBL.

5. Analysis of VITA structures

The basic part of analysis was performed in four measuring locations described in Table 1. For each plane the individual time averaging window of running variance T was determined using the maximum number of detections $N(+)$ criterion. The analysis performed for various distances from the wall confirmed that T maintained constant value within the entire logarithmic zone, while in the wall vicinity and at the edge of boundary layer the time window T varied slightly. For the convenience it was decided to keep the same T value across the whole boundary layer. The first important quantity i.e. the change of the bursting frequency, is presented in Fig. 6 as a number of detected structures N in y^+ coordinates for four consecutive measuring locations from Table 1. Each of the graphs represents the particular type of detected structures i.e. ascending

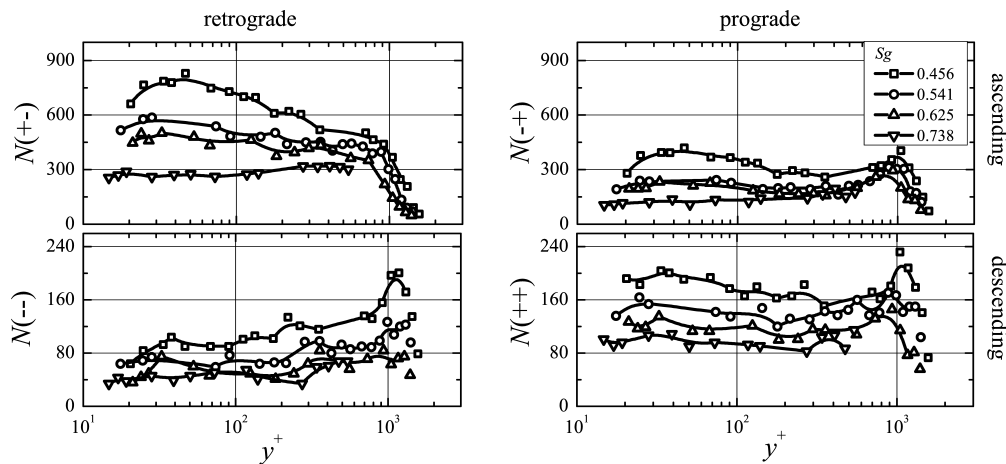


FIG. 6. Number of events N in y^+ coordinate along the APG flow for detection of: $(+)$, $(-)$ retrograde vortices, and $(-)$, $(+)$ prograde vortices.

vortices in the upper row, descending in the lower row, retrograde vortices in left column and prograde vortices in right column.

Figure 6 shows that number of detections is different for each type of structures. The dominant structure is the retrograde ascending one, almost two times lower number of detections was observed for prograde ascending and even less were found for prograde descending structures. Retrograde descending structures are by far the least frequent in the flow. Number of detections for each type of the structures decreases with the increasing distance from the wall, except for the retrograde descending ones. At the edge of boundary layer, the four types of structures are equally frequent. The number of structures detected decreases along the flow and the more pronounced decrease is observed for $N(+ -)$ i.e. for retrograde ascending vortex in the inner part of boundary layer ($y^+ < 200$).

It is obvious that the number of ascending structures is higher than the number of descending ones and their ratio is different for retrograde and prograde vortices. The detailed data are given in Fig 7, where the ratios of descending to ascending detections along y^+ coordinate for consecutive cross-sections are presented, the retrograde (Fig. 7a) and prograde (Fig. 7b) vortices are shown separately. It may be seen (Fig. 7a), that the $N(--)/N(+ -)$ ratio does not change significantly from one cross-section to another. For all cross-sections analysed the $N(--)/N(+ -)$ ratios are pretty close and they increase slightly across the boundary layer thickness and only at the edge of boundary layer a rapid jump is observed. Such a similarity of $N(--)/N(+ -)$ for consecutive cross-sections is not observed for prograde vortices (Fig. 7b), which are much less frequent in the flow, however the rapid jump is also visible at the outer edge of boundary layer. For prograde vortices the $N(++)/N(- +)$ ratio increases near the wall, which means that under the influence of APG the change of the vortex motion from ascending to descending appears. For both the prograde and retrograde

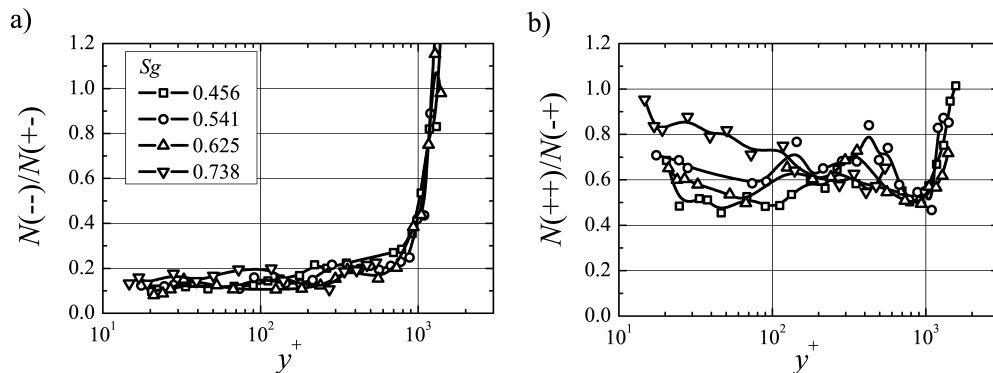


FIG. 7. Ratio of descending to ascending structures for: a) retrograde and b) prograde vortices.

ratios, unity at the edge of boundary layer is exceeded, which means that more descending than ascending vortices are detected.

The data presented in Fig. 6 suggest the decrease in the number of vortices detected in consecutive cross-sections, what in turn indicates, that the bursting frequency diminishes under APG conditions. The smaller number of bursts in unit of time should result in smaller contribution of organized structures to the overall energy of velocity fluctuations. To confirm this statement, the contributions from the detected structures to the long-time average of velocity fluctuations were calculated across the boundary layer for consecutive cross-sections. For this purpose, the integration time window was assumed to be an average time interval between the detected structures, which is substantially bigger than the length of window of running variance T , which characterizes the size of VITA structures. Figure 8a presents the contribution of coherent structures to overall energy of velocity fluctuations, which was calculated as the ratio of rms of phase averaged $\langle u \rangle$ and $\langle v \rangle$ fluctuations to the total rms of u' and v' of velocity fluctuations. The downstream evolution of $\langle u \rangle$ and $\langle v \rangle$ phase averaged velocity fluctuations is presented in Fig. 8b as a function of y^+ coordinate for four consecutive cross-sections. Figure 8a shows that the ratio $\langle u' \rangle / u'$ has a constant value at level of about 45% across the boundary layer except for the boundary layer edge, where the fast increase and then decrease of the coherent structures contribution is observed. It is due to the action of large-scale vortices few times larger than VITA structures, passing through the measuring point, which at first cause the increase, and then the decrease of instantaneous velocity. The phase integration time window are detected within the temporary velocity deficit, which cause the increase of $\langle u' \rangle$ magnitude.

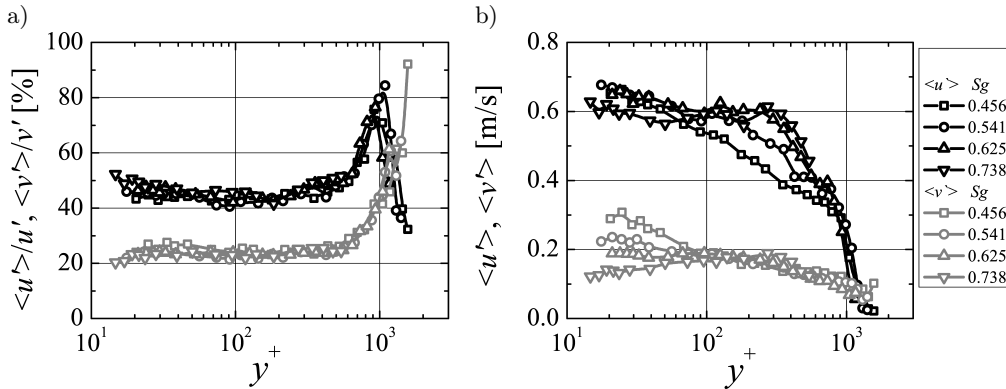


Fig. 8. Contribution of coherent structures to a) overall fluctuation intensity $\langle u' \rangle / u'$ and $\langle v' \rangle / v'$, b) evolution of phase averaged velocity fluctuations $\langle u' \rangle$ and $\langle v' \rangle$ along the flow.

As can be seen in Fig. 8a, the $\langle v' \rangle / v'$ ratio remains at the constant level equal to 25% across the boundary layer and only at the edge of boundary layer it lifts-

up sharply, what is the result of the large scale vortices action. This picture does not change along the flow from the first to the last cross-section, which means that bursting process governs the production of turbulence not only near the wall but also as high as to the end of logarithmic zone. When the interrogation area is moving downstream, the $\langle u' \rangle$ and $\langle v' \rangle$ distributions presented in Fig. 8b reveal a small decrease of both values in the inner layer (below $y^+ \approx 80$) and their increase in the outer layer (above $y^+ \approx 80$); this tendency is more distinct for $\langle u' \rangle$. One can conclude that those distributions are similar to distribution of $u'u'$ and $v'v'$ presented in Fig. 5. It is worth to note that the values of both $\langle u' \rangle / u'$ and $\langle v' \rangle / v'$ presented in Fig. 8a near the wall are relatively low in comparison with the results given by KIM *et al.* [3], who showed that fraction of one-dimensional mean square turbulent energy was in the range 0.6–0.7 in near-wall region. The reason for underestimation of near-wall phase averaged turbulent kinetic energy, is the applied length of integration time window, which in the present experiment corresponded to mean time interval between detections and was twice as long as the time window applied by KIM *et al.* [3]. The longer integration time window applied in the present experiment has a clear advantage, which is the ability to compare contributions of coherent structures $\langle u' \rangle / u'$ and $\langle v' \rangle / v'$ at different locations along the flow. The mean time interval between detections, inversely proportional to the number of structures, has an impact on the level of $\langle u' \rangle$ and $\langle v' \rangle$ fluctuations. The presented analysis confirms, that the turbulent kinetic energy production is closely related to the presence of coherent structures and that APG conditions have a distinct impact upon the intensity of bursting process. In particular one may conclude that the bursting process is damped near the wall (where the first maximum of fluctuations occurs) and enhanced in the logarithmic zone of boundary layer where the second maximum of fluctuations is located.

The next step of investigations was the detailed analysis of APG impact on phase averaged distributions of velocity components during the passage of detected VITA structures, which were performed for two distances from the wall i.e. $y^+ \approx 21$ and $y^+ \approx 180$, which are located close to the inner and outer maxima of velocity fluctuations respectively. Figure 9 shows the evolution of conditionally averaged traces of $\langle u \rangle$ and $\langle v \rangle$ on four graphs, that correspond to four types of detected structures. The same types of structure are placed on the same graph i.e. ascending vortices in the upper row, descending in the lower row, retrograde vortices in left column and prograde vortices in right column. Numbers of detected structures are presented in the legend at each graph.

Time τ was normalized by viscous time scale, because bursting process originates near the wall and all the compared structures may have the same scale across the boundary layer thickness. The particular plots give the evidence that

$Q2$ and $Q4$ are the characteristic events for ascending structures, while $Q1$ and $Q3$ are typical for descending structures. Furthermore, scaling by the viscous time scale revealed that the same size of vortices in τ^+ units has been obtained for all locations.

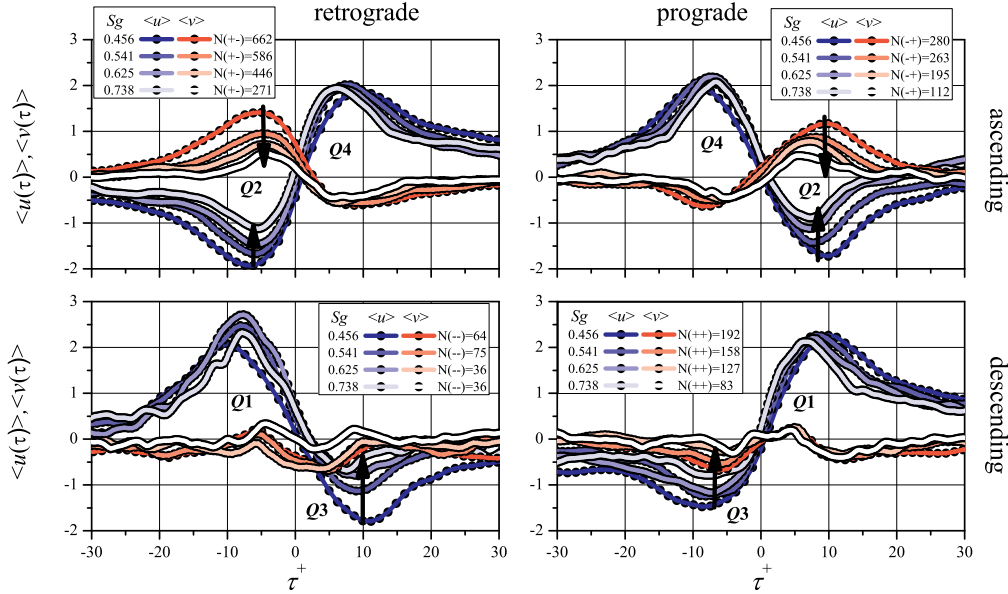


Fig. 9. Phase averaged velocity components recorded at $y^+ \approx 21$ (vicinity of inner peak) along APG flow: retrograde structures – left column, prograde – right column, ascending – upper row, descending – lower row. Arrows indicate changes along the flow.

One can observe that for measuring point located at $y^+ \approx 21$ (Fig. 9), the amplitude of $\langle u \rangle$ fluctuations are significantly larger in comparison with $\langle v \rangle$ and this observation holds for all four types of structures and all the cross-sections analysed. One should notice however, that the difference between $\langle u \rangle$ and $\langle v \rangle$ amplitudes depends upon the type of structure and for $y^+ \approx 21$ it is much more pronounced for descending structures. The next important quantity which should be analysed is the rate of decay of particular portions of $\langle u \rangle$ and $\langle v \rangle$ time-courses, which indicates the rate of decay of specific events. It is clear that the amplitude of $Q2$ event decreases under APG flow, which is seen as a drop of $\langle u \rangle$ and $\langle v \rangle$ amplitudes for ascending structures. A similar behaviour is seen for descending structures, where the activity of $Q3$ diminishes (Fig. 9). This means the increasing role of $Q4$ and $Q1$ events under APG flow. These observations are in line with remarks of KROGSTAD and SKARE [7], who concluded that for APG conditions the flow near the wall is dominated by strong $Q4$ and $Q1$ motions. The authors did not give, however, a clear explanation for this phenomenon as

their detection relied on the Reynolds uv shear stresses and they detected only these Q -type events.

As it results from the present investigations, $Q2$ and $Q3$ events disappear because in the APG flow near the wall the mean velocity significantly decreases, but the velocities of vortices do not follow the mean velocity because of their inertia, which delays their reaction on mean flow deceleration (see comments to Fig. 4). This phenomenon is responsible for the decay of $Q2$ and $Q3$ events for ascending and descending structures respectively.

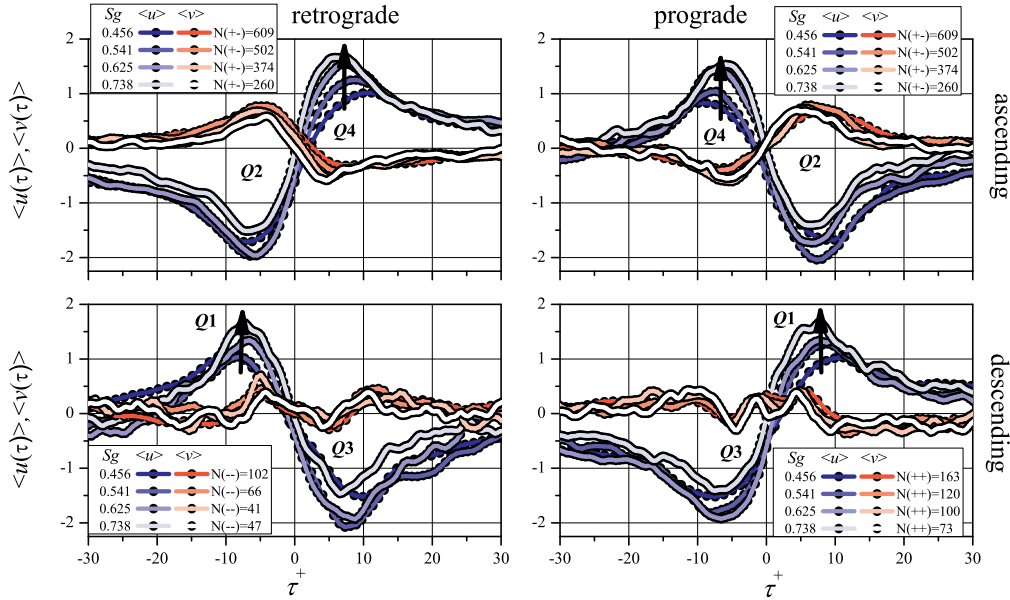


Fig. 10. Phase averaged velocity components recorded at $y^+ \approx 180$ (vicinity of outer peak) along APG flow: retrograde structures – left column, prograde – right column, ascending – upper row, descending – lower row. Arrows indicate changes along the flow.

Figure 10 shows the phase-averaged distributions for $y^+ \approx 180$ presented in the same manner as in Fig. 9. A similar amplitude of $\langle u \rangle$ for all types of structures is also observed like for the previous case, also the shape of $\langle v \rangle$ is similar. One may notice that for $y^+ \approx 180$, the presence of APG induces the increase of $\langle u \rangle$ amplitude, while $\langle v \rangle$ has a much smaller amplitude. These changes, however, translate into an increase of mean average $u'u'$ and $u'v'$ observed in Fig. 5. The shifts of $\langle u \rangle$ and $\langle v \rangle$ velocity components are not so strong for this case. However, the increase of $Q4$ and $Q1$ events are also visible.

The analysis of Figs. 9 and 10 confirms that APG conditions strongly influence the intensity of bursting process by damping it near the wall and enhancing it in the outer part of a boundary layer.

6. Conclusions

The analysis of turbulent, organised structures within the boundary layer with the use of VITA technique was performed. The paper gives an evidence of four types of vortical structures present in the TBL, which are responsible for the production of Q -type events. Namely, prograde and retrograde vortices, with the ascending and descending direction of motion were detected. It was observed that the number of detections decreases along the flow and this concerns all VITA structures, but is especially evident for retrograde ascending vortices, which appear near the wall. At the same time, in the presence of APG, the energy of those vortices near the wall decay along the flow, what explains the change in distributions of mean velocity fluctuations and confirms a less pronounced contribution of near-wall region to the downstream development of TBL. In parallel, the higher energy is produced by bursting process in outer region of turbulent boundary layer where outer maximum of velocity fluctuations is observed.

Quadrant analysis proved earlier findings of KROGSTAD and SKARE [7], namely the increased production of $Q4$ and $Q1$ events what coincides with decay of $Q2$ and $Q3$ events under APG condition. The reason of higher production of $Q1$ event according to KROGSTAD and SKARE [7], was the conversion of $Q4$ into the $Q1$ event, because of the wall redirecting the high speed fluid ($Q4$ event) away from the wall. Analysis presented in this paper allows to propose other explanation, namely that the delayed reaction of vortical structures on mean velocity decrease is responsible for the enhancement of $Q4$ and $Q1$ events of ascending and descending structures respectively, especially in the near-wall region. Due to higher vortex velocity of descending structures in comparison with the mean flow, the amplitude of $Q1$ event is higher than the amplitude of $Q4$ for ascending structures. In addition, the increased production of $Q1$ events (which produce the positive Reynolds stresses) near the wall is due to the lower number of descending vortices in comparison with the ascending ones.

Acknowledgements

The investigations presented in this paper have been obtained within the Grant No.: N N501 098238 (2010–2011) as well as European Social Funding project no.: POKL. 04.01.01-00-059/08, (2009–2010).

References

1. R.F. BLACKWELDER, R.E. KAPLAN, *On the wall structure of the turbulent boundary layer*, J. Fluid Mech., **76**, 89–112, 1976.
2. T. TEODORSEN, *Mechanism of turbulence*, [in:] Proc. 2nd Midwestern Conference on Fluid Mechanics, Ohio State University, Columbus, Ohio, 1–19, 1952.

3. H.T. KIM, S.J. KLINE, W.C. REYNOLDS, *The production of turbulence near a smooth wall in a turbulent boundary layer*, J. Fluid Mech., **50**, 133–160, 1971.
4. E.R. CORINO, R.S. BRODKEY, *A visual observation of the wall region in turbulent flow*, J. Fluid Mech., **37**, 1–30, 1969.
5. R.J. ADRIAN, *Hairpin vortex organization in wall turbulence*, Phys. Fluids, **19**, 041301, 2007.
6. V.K. NATRAJAN, Y. WU, K.T. CHRISTENSEN, *Spatial signatures of retrograde spanwise vortices in wall turbulence*, J. Fluid Mech. **574**, 155–167, 2007.
7. P.A. KROGSTAD, P.E. SKARE, *Influence of a strong adverse pressure gradient on the turbulent structure in boundary layer*, Phys. Fluids, vol. 7, No 8, 1995.
8. M. MATERNY, A. DRÓZDŹ, S. DROBNIK, W. ELSNER, *Experimental analysis of turbulent boundary layer under the influence of adverse pressure gradient*, Arch. Mech., **60**, 449–466, 2008.
9. S. DROBNIK, W. ELSNER, A. DRÓZDŹ, M. MATERNY-LATOS, *Experimental analysis of turbulent boundary layer with adverse pressure gradient corresponding to turbomachinery condition*, Proc. of Workshop “Progress in wall turbulence: understanding and modelling”, 21–23 April, Springer, 141–148, 2009.
10. F.J. KELLER, T. WANG, *Effects of criterion functions on intermittency in heated transitional boundary layers with and without streamwise acceleration*, Trans. of ASME, **117**, January 1995.
11. R.J. ADRIAN, C.D. MEINHART, C.D. TOMKINS, *Vortex organization in the outer region of the turbulent boundary layer*, J. Fluid Mech., **422**, 1–54, 2000.
12. M. ICHIMIYA, I. IKUO NAKAMURA, S. YAMASHITA, *Properties of a relaminarizing turbulent boundary layer under a favorable pressure gradient*, Experimental Thermal and Fluid Science, **17**, 37–48, 1998.
13. M. STANISLAS, J. JIMENEZ, I. MARUSIC, *Progress in Wall Turbulence: Understanding and Modeling*, Springer ERCOFTAC Series, Vol. 14, 2010.

Received September 17, 2010, revised version March 16, 2011.
